



STRUCTURAL AND ELECTRICAL MEASUREMENTS IN Mg²⁺ AND LA³⁺ Doped Co-Zn-Fe-O FERRITE NANOPARTICLES.



L. A. Dhale¹, K. A. Ganure² and K. S. Lohar³

¹Chemistry Department, Shrikrishan College, Gunjoti, Tq. Omerga, Maharashtra.

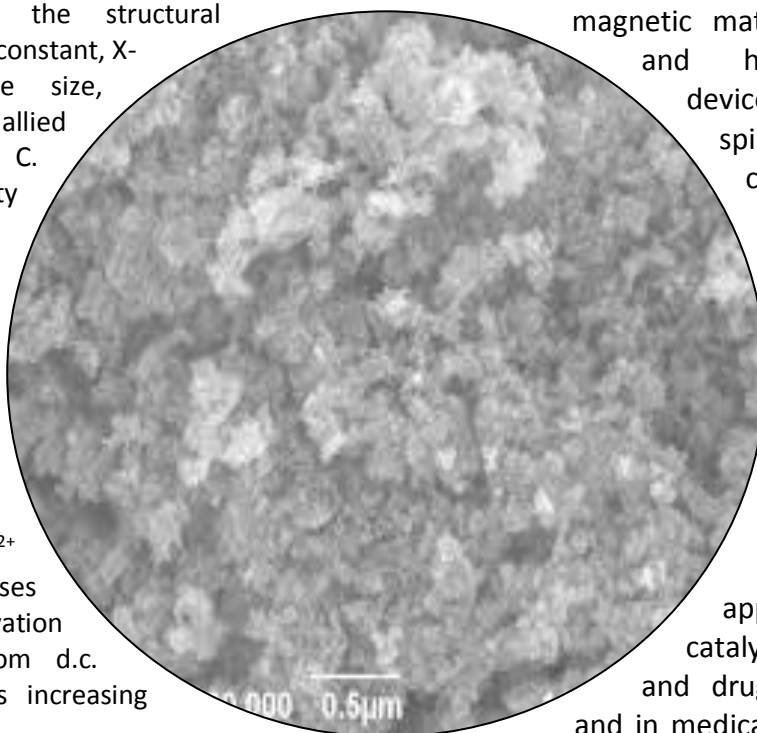
ABSTRACT :

Ferrite powders with chemical composition $Mg_xCo_{0.3}Zn_{0.7-x}Fe_{2-y}La_yO_4$ for $x = 0.1$ to 0.5 in the step of 0.1 and $y = 0.0$ to 0.1 in the step of 0.025 were synthesized by the sol-gel auto-combustion method. The structural and electrical properties of the synthesized ferrites were investigated. X-ray diffraction technique were used to determine the structural parameters like lattice constant, X-ray density, particle size, hopping lengths and allied parameters. D. C. electrical resistivity measurements were taken by using two probe techniques. The hopping lengths 'L_A' and 'L_B' are found to increase with increase in Mg²⁺ and La³⁺ concentration. The d.c. resistivity decreases as the Mg²⁺ and La³⁺ content increases as well as the activation energy calculated from d.c. resistivity plots shows increasing trend.

KEYWORDS: Hopping lengths, d.c. resistivity, activation energy.

INTRODUCTION

The great attention has focused on the preparation and characterization of super paramagnetic metal oxide nanoparticles of spinel ferrites, MFe_2O_4 (M = Co, Mg, Mn, Ni, etc.) [1]. The spinel ferrites are widely used magnetic materials in low cost and high performance devices. Nano crystals of spinel ferrite, a class of complex oxides, are under intense investigation to design with improved properties and for widespread applications. [2]. Ferrite nanoparticles find important applications in catalysis, data storage, and drug delivery systems and in medical diagnostics [3-6]. Nanosize particles of ferrites can be prepared using various synthesis techniques like hydrothermal [7], solid state [8] microemulsions [9] and other chemical methods [10]. among these various preparation methods of the ferrite



nanoparticles, the sol-gel auto-combustion Sol gel technique thermally induced anionic redox reaction takes place, to form exothermic reaction between oxidant and reluctant with high enough desirable phase with a very short time [11]. Co-Zn ferrite has attracted to the research interest based on its fascinating magnetic properties and potential applications in the field. Co-Zn ferrites are highly sensitive to temperature [12]. In the present paper we report the structural and electrical studies on $Mg_xCo_{0.3}Zn_{0.7-x}Fe_{2-y}La_yO_4$ prepared via sol-gel method.

Experimental:

Ferrite powders of composition $Mg_xCo_{0.3}Zn_{0.7-x}Fe_{2-y}La_yO_4$ for ($x = 0.1, 0.2, 0.3, 0.4, 0.5$ and $y = 0.0, 0.025, 0.05, 0.075, 0.1$) were synthesized by the sol-gel auto-combustion method. A.R. grade Magnesium Nitrate ($Mg(NO_3)_2 \cdot 6H_2O$), Cobalt Nitrate ($Co(NO_3)_2 \cdot 3H_2O$), Zinc Nitrate ($Zn(NO_3)_2 \cdot 6H_2O$), Lanthanum Nitrate ($La(NO_3)_3 \cdot 9H_2O$), Ferric Nitrate ($Fe(NO_3)_3 \cdot 9H_2O$), and Citric acid ($C_6H_8O_7 \cdot H_2O$) were dissolved in distilled water to obtain a mixed solution. The reaction procedure was carried out in an air atmosphere without the protection of inert gases. The molar ratio of metal nitrates to citric acid was 1:3. The metal nitrates were dissolved together in the minimum amount of double-distilled water needed to obtain a clear solution. An aqueous solution of citric acid was mixed with the metal-nitrate solution, and ammonia solution was slowly added to adjust the pH to 7. The mixed solution was placed on a hot plate with continuous stirring at 90 °C. During evaporation, the solution formed a very viscous brown gel. When all of the water molecules were removed from the mixture, the viscous gel began to froth. After few a minutes, the gel ignited and burnt with glowing flints. The decomposition reaction continued until the entire citrate complex was consumed. The auto-combustion was completed within a minute, yielding brown-colored ashes referred to as the precursor. The as-prepared powders of all the samples were sintered at 600 °C for 4 h to obtain the final product.

The samples were powdered for X-ray investigations. Part of the powder was X-ray examined by Phillips X-ray diffractometer (Model 3710) using Cu-K α radiation ($\lambda = 1.5405 \text{ \AA}$). The scanning step was 0.02° and scanning rate was 2 °/min. The d.c. resistivity measurements were taken by using two probe technique. The measurements were taken as a function of temperature in the temperature range 300 – 800 K. The measurements were taken in the step of 10⁰ of temperature.

Results and Discussion:

1. Structural Analysis:

Structure and composition of precursor particles were characterized by powder X-ray diffractometer (XRD). typical X-ray diffraction (XRD) pattern of the sample of $Mg_xCo_{0.3}Zn_{0.7-x}Fe_{2-y}La_yO_4$ ($x = 0.3$ and $y = 0.05$) shown in Fig. 1 represents the X-ray diffraction patterns of the ferrite samples at different Mg²⁺ and La³⁺ substitution. The reflection from the planes (2 2 0), (3 1 1), (2 2 2), (4 0 0), (4 2 2), (3 3 3) and (4 4 0), appeared for all the samples. This reveals that these samples are spinel ferrites and have only single cubic phase structure. The alloy formation is confirmed from the shift of XRD peak positions (Fig. 1). All samples possess the cubic spinel structure for each composition with the appearance of weak peaks as secondary phases ($LaFeO_3$, JCPDS card number 75-0541) for $x > 0.05$. An increase in La³⁺ substitution helps the formation of orthoferrite ($LaFeO_3$)

[13] with respect to those of the constituent pure phases. When an alloy is formed of two elements with similar crystal structure (isomorphism system), the lattice parameter is different from those of pure metals and the shift is a measure of the amount of the elements present. As the XRD peak positions are representative of the crystal structure and lattice parameters, a quantitative analysis can be carried out

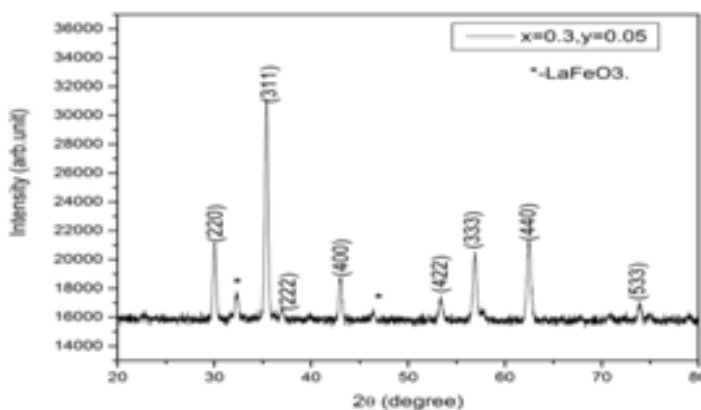


Fig. 1: Typical X-ray diffraction pattern of Mg_xCo_{0.3}Zn_{0.7-x}Fe_{2-y}La_yO₄ for x = 0.3, y=0.05.

The lattice constant ‘a’ of all the samples was determined by using the relation discussed elsewhere [14]. Lattice constant increases with increasing Mg²⁺ and La³⁺ substitution.

The X-ray density ‘d_x’ was calculated by using the following relation [15],

$$d_x = \frac{8M}{Na^3} \tag{1}$$

Where M is molecular weight, N is Avogadro’s number and ‘a’ is lattice constant. The X-ray density is found decrease increases with increase in Mg²⁺ and La³⁺ ion ferrite system. The particle size ‘t’ of the samples were calculated by using Scherer equation [14] and the particle size is obtain in the few nanometer range.

Distance between magnetic ions (jump lengths) in tetrahedral A-site and octahedral B-site i.e. ‘L_A’ and ‘L_B’ respectively is given by:

$$L_A = a \frac{\sqrt{3}}{4} \tag{2}$$

$$L_B = a \frac{\sqrt{2}}{4} \tag{3}$$

The variation of hopping lengths with composition x is shown in Fig. 2 and values are given in Table 1. It is evident from Fig. 2 that hopping length L_A and L_B both increased with increase in Mg²⁺ and La³⁺ ion substitution increases. This behaviour of hopping length with Mg²⁺ and La³⁺ substitution is suggest that jumping probability of ions are increases.

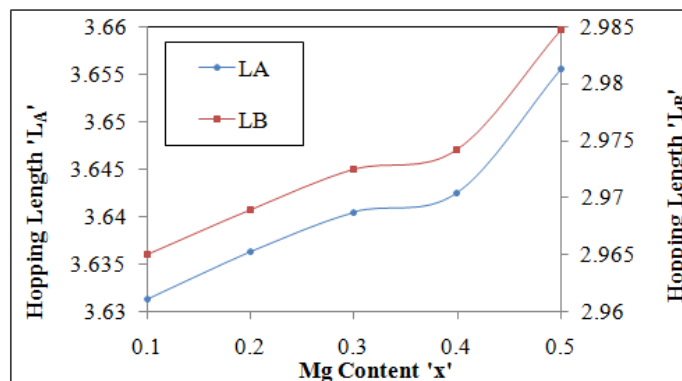


Fig. 2: Variation of hopping lengths(L_A and L_B) with Ce³⁺ composition x of Mg_xCo_{0.3}Zn_{0.7-x}Fe_{2-y}La_yO₄

Using the experimental values of lattice constant ‘a’, oxygen positional parameter ‘u’ and substituting using the equations discussed elsewhere [16], the allied parameters such as tetrahedral and octahedral bond length (d_{AX} and d_{BX}), tetrahedral edge, shared and unshared octahedral edge (d_{AXE}, d_{BXE} and d_{BXEU}) were calculated. The values of all the allied parameters are given in Table 1. It is observed that all the allied parameter increases with Mg²⁺ and La³⁺ substitution increases.

Table 1: Hopping length L_A and L_B, Tetrahedral bond (d_{AX}), octahedral bond (d_{BX}), tetra edge (d_{AXE}) and octahedral edge (d_{BXE}) (shared and unshared) of Mg_xCo_{0.3}Zn_{0.7-x}Fe_{2-y}La_yO₄.

Comp. x	Comp. y	Hopping length		d _{AX} (Å)	d _{BX} (Å)	Tetra edge d _{AXE} (Å)	Octa edge d _{BXE} (Å)	
		L _A (Å)	L _B (Å)				Shared	unshared
0.1	0.0	3.6313	2.965	1.902	2.047	3.107	2.822	2.966
0.2	0.025	3.636	2.968	1.905	2.050	3.114	2.826	2.970
0.3	0.050	3.640	2.972	1.907	2.052	3.115	2.829	2.974
0.4	0.075	3.642	2.974	1.908	2.053	3.116	2.831	2.975
0.5	0.1	3.655	2.984	1.915	2.061	3.128	2.841	2.986

2. Electric properties:

D.C Resistivity :

The electrical properties of the ferrite materials are tuneable as they depend on the chemical composition, preparation method, sintering temperature type of dopant etc. Properties like electrical conductivity give the valuable information about conduction mechanism. In general, the conductivity of spinel ferrites is due to the presence of Fe²⁺ ions. The conductivity arises due to mobility of extra electron, which comes from Fe²⁺ through the crystal lattice [17]. The movement is described by a hopping mechanism, in which the charge carriers jump from one ionic site to the next [18]. The d.c. electrical resistivity of all the samples by varying temperature were measured by using two probe method in the temperature range 300-800 K. the measurements were recorded in

the step of 10K. The resistivity of all the samples was determined by using the Arrhenius relation [19].

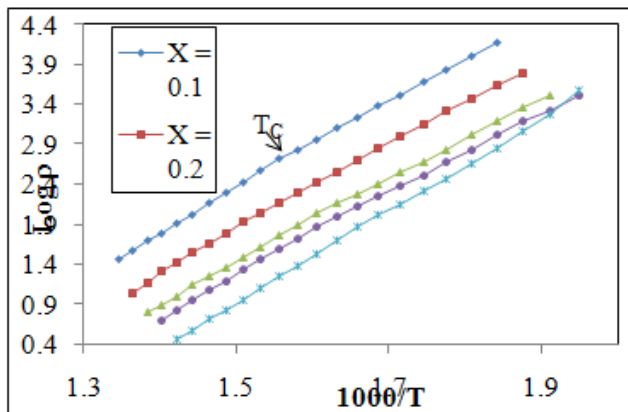


Fig. 3: Variation of log ρ versus 1000/T for the series Mg_xCo_{0.3}Zn_{0.7-x}Fe_{2-y}La_yO₄.

$$\rho = \rho_0 e^{\left(\frac{-E_g}{kT}\right)} \quad (4)$$

Where, ρ is resistivity, E_g is activation energy, T is temperature, k Boltzmann constant

The temperature dependence of D.C. electrical resistivity of Mg-La substituted Co-Zn ferrite is shown in Fig. 3. It is observed from Fig. 3, that the ferrites have semiconducting nature, where the D.C. electrical resistivity decreases on increasing the temperature [20]. The values of activation energy for paramagnetic region and ferrimagnetic region and the transition temperatures for all the samples are summarized in Table 2. It is observed from Table 2, that activation energy for paramagnetic region is more as compared to ferrimagnetic region. The conduction mechanism in these ferrites can be explained on the basis of hopping of polarons.

Table 2: Transition temperature (T_c) and activation energy (ΔE) for Mg_xCo_{0.3}Zn_{0.7-x}La_yFe_{2-y}O₄.

Comp. 'x'	Comp. 'y'	Transition Temperature 'T _c ' (K)	Activation energy (eV)		
			E _p	E _f	ΔE
0.1	0.0	639	5.8872	5.1823	0.705
0.2	0.025	627	5.8409	5.1239	0.717
0.3	0.05	614	5.7602	5.0212	0.739
0.4	0.075	609	5.7321	4.9848	0.747
0.5	0.1	598	5.7276	4.9350	0.793

CONCLUSIONS:

The substitution of Mg^{2+} and La^{3+} ions in Co-Znferrite synthesized by sol gel Autocombunation techniques. Hopping length L_A and L_B both increasing to increase. The Allied parameter increase to increase the Mg^{2+} and La^{3+} ions. The d.c. resistivity decreases as the Mg^{2+} and La^{3+} concentration increases. The activation energy calculated from slopes of para and ferri region shows increasing trend. This nature of activation energy can be explained on the basis of hopping of polarons.

REFERENCES:

1. Y. Köseog˘lu , A. Baykal , F. Gözüak , H. Kavas . Polyhedron. 28 (2009) 2887–2892.
2. Sanjeev Kumar, Vaishali Singh, SarojAggarwal, Uttam Kumar Mandal, and Ravinder Kumar Kotnala. J. Phys. Chem. C, 114 (2010) 6272–6280
3. Kula Kamal Senapati, ChandanBorgohain, Prodeep Phukan., Journal of Molecular Catalysis A: Chemical ,339 (2011) 24–31
4. Y. Yin, A.P. Alivisatos, Nature 437 (2005) 664.
5. Tartaj P., Morales M. P., Verdaguer S., González-Carreño T., Serna C. J.; J. Phys. D: Appl. Phys. 36 (2003) R182.
6. Berry C. C, Curtis A. S. G ,J. Phys. D: Appl. Phys. 36 (2003) R198.
7. Rath C , Anand S , Das R. P, Sahu K. K , Kulkarni S. D , Mishra N. C, J. Appl. Phys. 91(2002)2211.
8. AzadehNajafiBirgani, Mohammad Niyafar,Ahmad Hasanpour. Journal of Magnetism and Magnetic Materials.374(2015)179–181
9. Maria YousafLodhi , Khalid Mahmooda, AzharMahmood , Huma Malik , Muhammad FarooqWarsi, Imran Shakir, M. Asghar , Muhammad Azhar KhanCurrent. Applied Physics ,14 (2014) 716-720.
10. Hyeon T. Chem. Commun. 8 (2003) 927.
11. Z.Yue .WenyuGuo. Ji Zhou, ZhilumGui. Longtu Li. Journal of magnetism and magnetic materials. 270 (2004) 216.
12. SanjeevKumar ,Vaishali Singh ,Uttam K. Mandal , R.K. Kotnala .InorganicaChimicaActa. 428 (2015) 21–26
13. Choudhari V. Shirsath S. E., Mane M. L., Kadam R. H., Shelke S. B., Mane D. R., Journal of Alloys and Compounds. 549(2013)213.
14. B. D. Cullity, Elements of X-ray diffraction (Addison – Wesley, USA)
15. A.V. Raut, R.S.Barkule, D.R.Shengule, K.M.Jadhav. Journal of Magnetism and Magnetic Materials .358-359(2014) 87–92.
16. Lohar K. S., Pachpinde A. M., Langade M. M., R. H. Kadam, S. E Shirsath., J. Alloys Comp. 604 (2014) 204.
17. MurthyV. R. K. Sobhanadri.J.Phys. Status Solidi.(1976)36:133
18. Ahmed I., Farid M. T., Kousar R., Niazi S. B. World Applied Sciences Journal,(2013) 22:796.
19. RezlescuE., Rezlescu N., Popa P. D., Rezlescu L., Pasnicu C., Phys. Sol (a) (1997) 162:673.

20. Sattar A. A., El-sayed H. M., El-Shokrofy K. M., El-tabey M. M., J. Appl. Sci. (2005) 5:162
21. Mazen S. A., Abdallah M. H., Sabrah B. A., Hashem A. M., Phys. Stat. Sol. (a) (1992) 134:263.